Ecological Archives **E000-000-A1**

Warming tolerance across insect ontogeny: influence of joint shifts in microclimates and thermal limits (S. Pincebourde and J. Casas).

Details on the biophysical model

The complete heat budget of a mine is explained in Pincebourde and Casas (2006). Here, we describe only the two terms containing stage-specific parameters: the net radiative heat budget and the latent heat term. All other parameters are given in Table 1 of Pincebourde and Casas (2006).

The net radiative energy budget (R_n, W m^{-2}), i.e., the amount of radiative energy actually absorbed by a mine at stage *i*, was calculated as:

[A.1] $$R_n = a_i^{VIS} I^{VIS} + a_i^{NIR} I^{NIR} + a_i^{TIR} \varepsilon_{env} \sigma T_{air}^4 - \varepsilon_i \sigma T_i^4$$

Where a_i^{VIS}, a_i^{NIR} and a_i^{TIR} are the absorbance values in the visible, near infrared, and thermal infrared ranges, respectively; I^{VIS} and I^{NIR} are the amount of radiation in the visible and near infrared range of the radiation spectrum; ε_{env} and ε_i are the emissivities (thermal infrared range of the spectrum) for the surroundings and the mine; T_{air} and T_i are the ambient air and mine temperatures, respectively; and σ is the Stefan Boltzmann constant (5.67 10^{-8} W m^{-2} K^{-4}). According to the Kirchhoff's law, absorbance in the thermal infrared range equals the emissivity. This value is around 0.97 for leaves, i.e. $a_i^{TIR} = \varepsilon_i = 0.97$ (Campbell and Norman 1998). We set the environmental emissivity ε_{env} to 0.90 as a standard to the walls of the Conviron chamber we used (see below). The activity of the leaf miner causes changes in absorbance values a_i^{VIS} and a_i^{NIR} (Pincebourde and Casas 2006).

The latent-heat equation computes the amount of heat lost during evapotranspiration in a mine at stage *i*, *E* (W m^{-2}):

[A.2] $$E=\lambda g_i^v\left(\frac{e_s\left(T_i\right)-e_a}{p_a}\right)$$

Here, λ is the latent heat of vaporization for water (λ = 44 kJ mol^{-1} at 25 °C), g_i^v is the leaf conductance for water vapour transfer (mol m^{-2} s^{-1}), $e_s\left(T_i\right)$ is the saturated water vapour pressure (Pa) at mine temperature T_i (°C), e_a is the water vapour pressure in the air (Pa) and p_a is the atmospheric pressure (=101.3 kPa). The term $e_s\left(T_i\right)-e_a$ corresponds to the mine water vapour pressure deficit (D_i). Equation (2) is based on the assumption that the internal atmosphere of a leaf or a mine is saturated for water vapour. This assumption is reasonable since relative humidity within the leaf atmosphere is higher than 95% (Nobel 1999). The leaf conductance for water vapour is computed by combining the boundary layer conductance and the tissue conductance (stomatal conductance and epidermis conductance). This computation integrates the Jarvis sub-model (Jarvis 1976) to calculate the stomatal conductance which directly influences the amount of water vapour that leaves the mine. According to the Jarvis sub-model, the effects of each environmental variable are multiplicative but the interactions are non-synergetic. Such simple multiplicative model does not necessitate knowledge on the mechanisms underlying stomatal behaviour (Damour et al. 2010), and the Jarvis model parameters are known for apple (Pincebourde and Casas 2006). The stomatal conductance in a mine at stage *i* (g_i^{vs}, mol m^{-2} s^{-1}) was computed as

[A.3] $$g_i^{vs}=g_i^{s\max}\,f_i^1\left(Q\right)f_i^2\left(D_i\right)f_i^3\left(T_i\right)$$

Where $g_i^{s\max}$ is the maximal stomatal conductance (mol m^{-2} s^{-1}), attained under specific levels of leaf irradiance (Q, µmol PAR m^{-2} s^{-1}), mine water vapour pressure deficit (D_i, Pa) and

mine temperature (T_i, °C). The functions f_i^1, f_i^2 and f_i^3 describe the variation in stomatal conductance relative to the maximal value following a change in leaf irradiance level, mine water vapour pressure deficit and mine temperature respectively. The leaf miner activity induces changes in these parameters (Pincebourde and Casas 2006). The response functions (f_i) are known for intact leaf tissues and L5 mines. For the temperature response function (f_i^3), which reach its maximal value at 19 °C, we set it constant and equal to 1 because (i) we measured the maximal stomatal conductance ($g_i^{s\max}$) at 25 °C, and (ii) it was noticed that stomatal conductance of L5 mines becomes unresponsive to temperature changes after $T_i = 25\,°C$ (Pincebourde and Casas 2006). For eggs and L4 mines, we used the functions of intact leaf tissues, while we applied the functions of mines for L5 larvae and pupae. These empirical functions are given in Pincebourde and Casas (2006).

Dynamics of absorbance during insect ontogeny

Absorbance in the visible (a_i^{VIS}) and near infrared (a_i^{NIR}) ranges of the solar spectrum are known for intact apple leaf tissues and L5 mines (Pincebourde and Casas 2006). These values, combined with the temporal dynamics of window formation, were used to infer absorbance values at the L4 and pupae stages. We followed three steps. Firstly, we determined the surface area of feeding windows for L4 mines (at 30% of L4-L5 development time), L5 mines (at 70% of L4-L5 development time) and pupae (at 100% of development time) using the logistic model mentioned above that describes the feeding dynamics. Secondly, we defined a linear relationship describing the change in absorbance as function of the surface area of feeding windows using the known absorbance values for intact leaf tissues and for L5 mines. Third, absorbance values for L4 mines and pupae were interpolated using this linear model. The linear equations relating absorbance in the visible (a^{VIS}) and near infrared (a^{NIR}) were

[A.4] $a^{VIS} = -0.0148\, S^{FW} + 0.8425$

[A.5] $a^{NIR} = 0.0149\, S^{FW} + 0.0247$

Where S^{FW} is the percentage of total mine surface area corresponding to feeding windows. This method assumes that the decrease in absorbance in the visible range is proportional to the decrease in the portion of green patches remaining in a mine, while the increase in absorbance in the near infrared range correlates with the increase in the portion of feeding windows.

Dynamics of stomatal conductance during insect ontogeny

The latent heat term of the biophysical model was parameterized by measuring the maximal stomatal conductance ($g_i^{s\max}$) at egg stage (intact leaf tissues), and L4, L5, and pupae mines. Gas exchange were measured with an infrared gas analyzer equipped with a 2×3 cm leaf chamber system (LI-6400, Li-Cor Inc., Lincoln, NE, USA) and with an external light source (6400-02B, Li-Cor Inc.). The conditions giving maximal stomatal conductance differs among stages. For eggs and L4, maximal values were obtained at leaf temperature 25 °C, VPD 1 kPa and irradiance 1500 µmol.m^{-2}.s^{-1}. By contrast, for L5 and pupae, it was temperature 19 °C, VPD 1 kPa and irradiance 600 µmol.m^{-2}.s^{-1}. We submitted L5 and pupae to these conditions except for temperature which was set to 25 °C for all. Indeed, stomatal conductance in old mines becomes unresponsive to temperature variations for temperature > 25 °C (Pincebourde and Casas 2006), and our simulations were all made at these higher temperatures (see below). We measured maximal stomatal conductance on 20 intact leaves (egg stage), 10 L4 mines, 20 L5 mines, and 14 pupae. A thin layer of vegetable oil was used to coat the leaf tissues adjacent to the mined area to measure gas exchange occurring only in the mine integument (Pincebourde et al. 2006). All measurements were made on pre-illuminated leaves, to ensure that stomata were active, and after an equilibration time of 20–30 min.

Microclimate temperature measurements

Microclimatic temperatures were recorded by placing apple seedlings containing leaf mines in a Conviron chamber (VB 1014-A, Vötsch, Balingen Frommern, Germany) which allowed full control of environment. Two metal halide lamps (250 W; Sylvania Britelux HSI-T SX clear) mimicked the solar spectrum. Radiation level was controlled by adjusting the distance between leaf surfaces and the bulbs. It was measured systematically for each leaf and mine using a pyranometer sensor (CM3, Campbell Scientific, Leicestershire, UK). A fine copper-constantan thermocouple (type T, 0.2 mm in diameter; TCSA, Dardilly, France), connected to a Campbell CR10X datalogger (Campbell Scientific), was used to measure microclimate temperatures. For eggs, the thermocouple was applied to the lower leaf surface next to an egg. For L4, L5, and pupae, the thermocouple was inserted within the mine through a feeding window (Pincebourde and Casas 2006). A drop of vegetable oil was used to fill the small hole around the thermocouple.

LITERATURE CITED

Campbell, G. S., and J. M. Norman. 1998. An introduction to environmental biophysics. Second Edition. Springer Verlag, New York, New York, USA.

Damour, G., T. Simonneau, H. Cochard, and L. Urban. 2010. An overview of models of stomatal conductance at the leaf level. Plant Cell and Environment 33:1419–1438.

Jarvis, P. G. 1976. The interpretation of the variations in leaf water potential and stomatal conductance found in canopies in the field. Philosophical Transactions of the Royal Society B 273:593–610.

Nobel, P. S. 1999. Physicochemical and environmental plant physiology. Second Edition. Academic Press, New York, New York, USA.

Pincebourde, S., and J. Casas. 2006. Multitrophic biophysical budgets: thermal ecology of an intimate herbivore insect-plant interaction. Ecological Monographs 76:175–194.

Pincebourde, S., E. Frak, H. Sinoquet, J. L. Régnard, and J. Casas. 2006. Herbivory mitigation through increased water use efficiency in a leaf mining moth-apple tree relationship. Plant Cell and Environment 29:2238–2247.

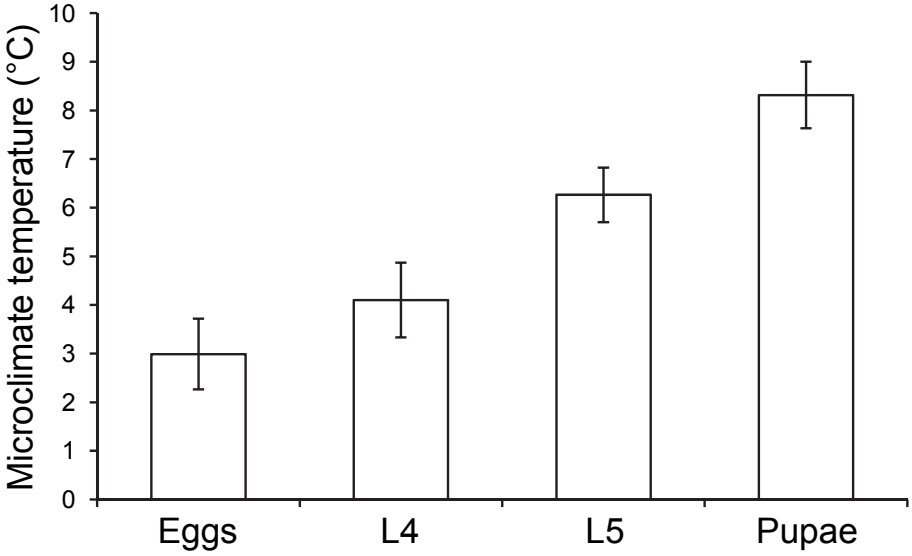

FIG. A1. Mean (±SD) microclimate temperature excess for each life stage under the same environmental conditions at air temperature 25 °C. The microclimatic temperature excess experienced by larvae and pupae within their mines differed markedly despite identical environmental conditions within the experimental chamber (ANOVA: $F_{3,39} = 159.17$, $P < 0.001$). The microclimatic temperature of eggs and L4 larvae were similar, at about 3–4 °C above ambient (Tuckey HSD multiple comparisons: $P = 0.012$). The subsequent stages experienced much warmer microclimates, at about 6 °C and 8 °C above ambient for L5 and pupae, respectively (Tuckey HSD multiple comparisons: $P < 0.001$ for all comparisons involving L5 and pupae).

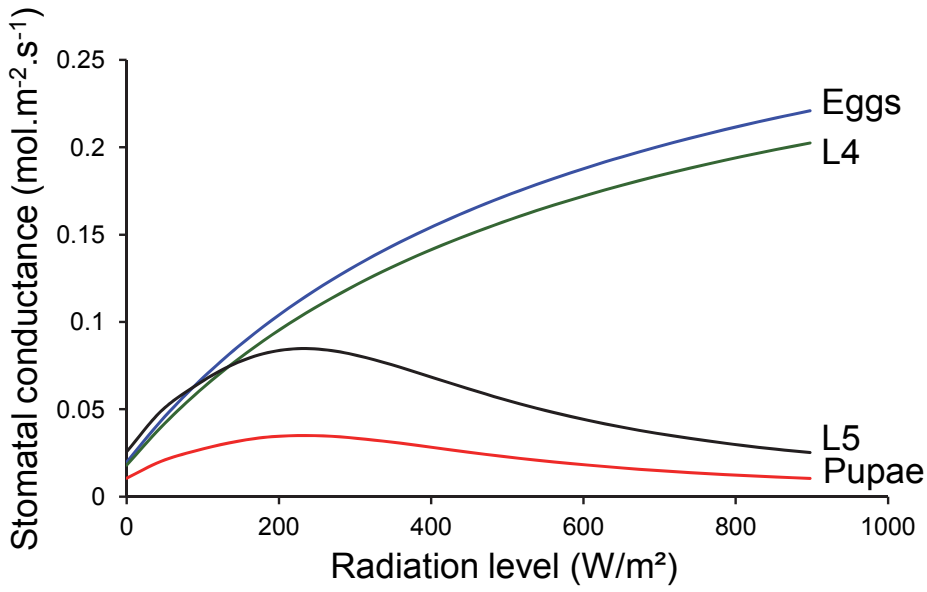

FIG. A2. Model simulation of stomatal conductance as function of radiation level at the leaf surface for each life stage. Stomatal closure appears clearly in the oldest stages (the pupae and L5).

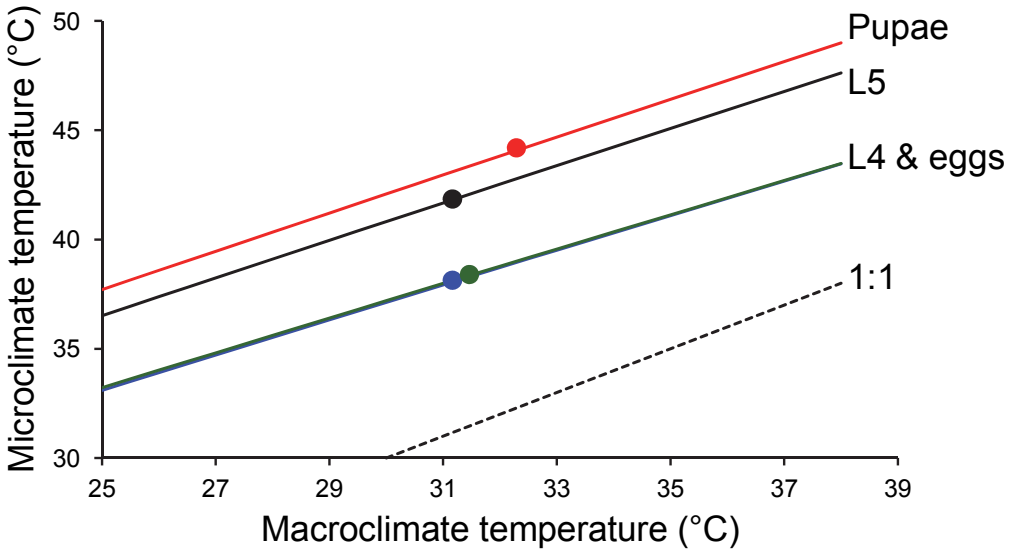

FIG. A3. Predicted microclimate temperature during warming for each life stage (colour lines). The dashed line represents equality (when microclimate and macroclimate temperatures are similar). Filled circles indicate the temperatures at which the upper lethal temperature is reach along the microclimate warming for each life stage.